Ocean Modelling xxx (2015) xxx–xxx

Contents lists available at ScienceDirect

Ocean Modelling

journal homepage: www.elsevier.com/locate/ocemod

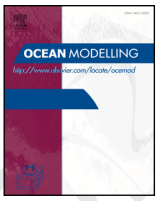

Virtual Special Issue
Ocean Surface Waves

Detection and analysis of coherent groups in three-dimensional fully-nonlinear potential wave fields

Q1 E.V. Sanina[a,*], S.A. Suslov[a], D. Chalikov[a,b], A.V. Babanin[a]

[a] Centre for Ocean Engineering, Science and Technology, Swinburne University of Technology, Melbourne 3122, Australia
[b] Institute of Oceanography RAS, Saint-Petersburg 199004, Russian Federation

ARTICLE INFO

Article history:
Received 12 January 2015
Revised 24 September 2015
Accepted 27 September 2015
Available online xxx

Keywords:
Nonlinear waves
Coherent wave groups
Velocity of groups

ABSTRACT

We investigate the emergence of coherent groups in three-dimensional fully-nonlinear potential deep water waves whose initial spectrum is assumed to be of the JONSWAP type with directional distribution given by $\cos^n\theta$, where n is the integer varying from 1 to 16. The analysis is based on the results of long-term wave simulations performed using a numerical solution of a three-dimensional Laplace equation for the velocity potential subject to nonlinear kinematic and dynamic boundary conditions at the free surface. The main characteristics of wave groups such as their average velocity, maximum group wave height, lifetime and length are analysed. The statistics of extreme waves occurring in the detected groups are discussed. Spatial and temporal scale characteristics of wave groups are compared to the previous results.

1. Introduction

Wave groups are apparent features of surface waves, whether those are observed in one-dimensional wave flume or in the two-dimensional ocean surface. Such groups are formed as result of linear (e.g. Longuet-Higgins, 1984) and nonlinear interactions (Benjamin and Feir, 1967), but their dynamics are yet to be fully understood, particularly, in the case of directional wave fields. In this paper we will investigate the observed properties of such groups produced by a three-dimensional wave model (Chalikov et al., 2014) described in Section 2, without discussing explicit dynamics responsible for their appearance.

The analysis of grouping properties of a wave field in space and time can be performed using various approaches. Traditionally, the wave elevation time series are acquired by in-situ sensors (i.e. anchored buoys, wave lasers) moored at a fixed position (Hamilton et al., 1979; Donelan et al., 1996). The alternative to the point measurements are remote sensing techniques capable of acquiring temporal sequences of images of the ocean surface. For instance, the techniques that are based on the use of passive sensors such as video cameras (Gallego et al., 2011; Benetazzo et al., 2012), microwave sensors and incoherent and coherent radars mounted on off- and on-shore stations or moving vessels can be applied (Nieto Borge et al., 2013). The mentioned methods have been used for the analysis of group features in many studies (e.g. Ziemer and Dittmer, 1994; Bell et al., 2006; Reichert and Lund, 2007, among others).

To detect coherent groups on the ocean surface obtained either from records or numerical simulations, the two-dimensional upper wave envelope (referred to as the envelope below) is constructed using various techniques: Riesz transform (King, 2009), Hilbert transform (Huang et al., 1999) or cubic spline approach described in Section 3. The fully developed coherent structures are typically visualised using the upper wave envelope because it is easier to be observed experimentally. Q2

The first attempt to detect the geometry of coherent structures in directional wave fields was made in Sanina et al. (2014). Here we develop this approach further. The spline-based approach for the one-dimensional groups is described in Section 3.2. It is extended to detect two-dimensional wave field structures combining one-dimensional groups as discussed in Section 3.3. The number of the groups detected is analysed using it in Section 4.1. Q3 The velocity of the detected groups is compared with the group velocity

$$c_g = \frac{1}{2}\sqrt{\frac{g}{k_p}} \tag{1}$$

of linear waves, where g is the gravity and k_p is the wavenumber of the wave spectrum peak (Section 4.2). Other features of the identified

* Corresponding author. Tel.: +61 478035962.
E-mail address: esanina@swin.edu.au, sanina.e.v@gmail.com (E.V. Sanina).

http://dx.doi.org/10.1016/j.ocemod.2015.09.012
1463-5003/

groups such as their lengths, lifetime and steepness are investigated in Sections 4.3, 4.4 and 4.5. The statistics of the occurrence of extreme waves in the groups is discussed in Section 4.5. In order to quantify the spatial and temporal wave group characteristics the space-time autocorrelation functions of the surface elevation envelopes are constructed using Hilbert transform (Section 5).

2. Numerical model of three-dimensional fully nonlinear potential periodic waves

We solve numerically the three-dimensional Laplace equation for the velocity potential $\phi(x, y, z, t)$

$$\frac{\partial^2\phi}{\partial x^2} + \frac{\partial^2\phi}{\partial y^2} + \frac{\partial^2\phi}{\partial z^2} = 0 \tag{2}$$

subject to the kinematic condition

$$\frac{\partial\eta}{\partial t} + \frac{\partial\eta}{\partial x}\frac{\partial\phi}{\partial x} + \frac{\partial\eta}{\partial y}\frac{\partial\phi}{\partial y} - \frac{\partial\phi}{\partial z} = 0 \tag{3}$$

and the dynamic condition

$$\frac{\partial\phi}{\partial t} + \frac{1}{2}\left(\left(\frac{\partial\phi}{\partial x}\right)^2 + \left(\frac{\partial\phi}{\partial y}\right)^2 + \left(\frac{\partial\phi}{\partial z}\right)^2\right) + \eta + p = 0 \tag{4}$$

at the free surface $z = \eta(x, y, t)$, where p the pressure created by the air flow above the surface and $\frac{\partial\phi}{\partial z} = 0$ at $z \to -\infty$, where (x, y, z) are the Cartesian coordinates and t is time. The equations are solved on a periodic domain bounded by the wave surface: $0 < x < 2\pi$, $0 < y < 2\pi$, $-\infty < z \le \eta(x, y, t)$. The variables ϕ and η are considered to be periodic in the x and y directions, and x is the main wave propagation direction.

Eqs. (2)–(4) are expressed in non-dimensional form, for which we introduced the scale $L = \frac{\lambda_p^*}{\lambda_p}$ for the x, y and z coordinates, where λ_p^* is the dimensional wavelength of the main wave, $\lambda_p = \frac{2\pi}{k_p}$ is the corresponding non-dimensional wavelength, k_p is the wavenumber in a non-dimensional computational domain. This choice ensures that the computational domain consists of k_p main waves. We also define the scale for the dimensional time t^* as $T = \sqrt{\frac{L}{g}}$, so that the $t^* = Tt$. Using these two scales the expression for the dimensional quantities ϕ^* and p^* in terms of non-dimensional ϕ and p becomes

$$\begin{aligned} \phi^* &= \frac{L^2}{T}\phi, \\ p^* &= \rho\frac{L^2}{T^2}p, \end{aligned} \tag{5}$$

where ρ is the density of water.

The numerical solution introduced in Chalikov et al. (2014) is obtained in the non-stationary surface-following non-orthogonal coordinate system

$$\xi = x, \quad \nu = y, \quad \zeta = z - \eta(\xi, \nu, t). \tag{6}$$

The equations in the curvilinear coordinates are Fourier-transformed in the horizontal directions and are discretised using central differences in the vertical direction. The obtained system of ordinary differential equations for Fourier coefficients is integrated in time using the 4th order Runge–Kutta method. The initial spectrum is assumed to be of the JONSWAP type with directional distribution given by $\cos^n\theta$, where n is integer.

3. Detection of wave groups

Here we describe two methods for constructing the upper envelope for unidirectional waves propagating in the x direction: Hilbert transform and the cubic spline approach. We will use them for different analysis tasks.

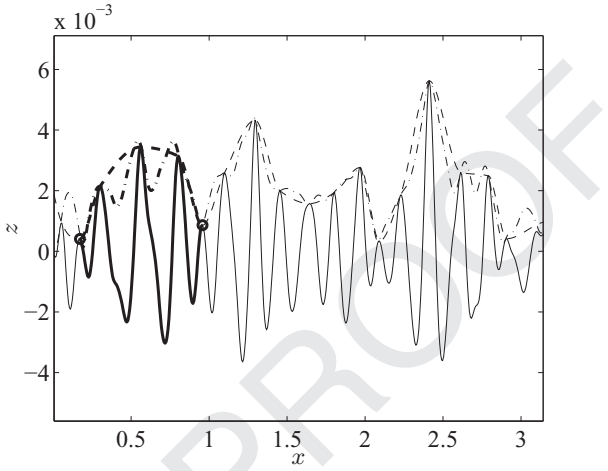

Fig. 1. Constructing a one-dimensional wave (solid line) upper envelope using Hilbert transform (dash-dotted line) and the directional cubic spline approach (dashed line). The thick line shows the group detected using a cubic spline.

3.1. Construction of a wave envelope using Hilbert transform

We denote a section of a wave surface $\eta(x, y, t)$ along the direction of a vector $\vec{l}$ in the (x, y) plane as $\eta_0(\vec{l}, t)$. The wave envelope, denoted as $\xi(\vec{l}, t)$, is defined in Huang et al. (1999) along the path L as

$$\xi = \sqrt{\eta_0^2 + \tilde{\eta}_0^2}$$

where $\tilde{\eta}_0$ is one-dimensional Hilbert transform of the free surface η_0

$$\tilde{\eta}_0 = \mathfrak{H}\{\eta_0\} = \int_L \frac{\eta_0(l', t)}{l - l'}\, dl', \tag{7}$$

where L is a linear path in the direction of $\vec{l}$.

The wave envelope ξ enables one to estimate the instantaneous local properties of the wave surface. Hence, assuming that the wave elevation $\eta_0(\vec{l}, t)$ can be treated as a random Gaussian process, its probability density function is given by Rayleigh distribution (Papoulis and Pillai, 2002). Assuming further that the wave elevation $\eta_0(\vec{l}, t)$ is a narrow-banded process (that is characterised by a narrow range of frequencies), the probability of maxima of $\tilde{\eta}_0$ being located more than a half of a wavelength away from the nearest wave crests is small. Hence, $\xi(\vec{l}, t)$ is strongly correlated with the amplitudes of individual waves. In addition, for narrow-banded processes, there is a statistical symmetry between crests and troughs. All of the above make Hilbert transform an efficient method for constructing the upper envelope and for its statistical analysis. However we found that this method has a number of disadvantages when wave groups need to be identified.

To describe them we first define a one-dimensional wave group as a part of the wave between the neighbouring minima of the wave envelope. We define the length of a wave group as the distance l between these minima. We only consider sufficiently long groups with

$$l > l_{min} = 4\lambda_p, \tag{8}$$

where λ_p is the main wave length, as we are interested in large coherent structures. It is seen from Fig. 1 that the envelope resulting from Hilbert transform shown by the dash-dotted line contains parasitic minima. This is a known problem. To address it filtering is commonly used after the envelope is constructed Longuet-Higgins (1984).

Please cite this article as: E.V. Sanina et al., Detection and analysis of coherent groups in three-dimensional fully-nonlinear potential wave fields, Ocean Modelling (2015), http://dx.doi.org/10.1016/j.ocemod.2015.09.012